Solar, Heliospheric and Ionospheric Physics: Pathfinders, Precursors and SKAO Perspectives

Pietro Zucca,[1] Rohit Sharma,[2] Divya Oberoi,[3] Eduard Kontar,[4] John Morgan,[5] Peter Gallagher,[6] Sven Wedemeyer[7,8] and Biagio Forte[9]

[1]*ASTRON - Netherlands Institute for Radio Astronomy, Oude Hoogeveensedijk 4, 7991 PD Dwingeloo, The Netherlands*
[2]*Indian Institute of Technology, Kanpur 208016, India.*
[3]*National Centre for Radio Astrophysics, Tata Institute of Fundamental Research, S. P. Pune University Campus, Pune, India*
[4]*Uni Glasgow*
[5]*CSIRO, Space and Astronomy, P.O. Box 1130, Bentley, WA 6102, Australia*
[6]*Astronomy & Astrophysics Section, School of Cosmic Physics, Dublin Institute for Advanced Studies, DIAS Dunsink Observatory, Dublin D15 XR2R, Ireland*
[7]*Rosseland Centre for Solar Physics, University of Oslo, Oslo, Oslo, N-0315, Norway*
[8]*Institute of Theoretical Astrophysics, University of Oslo, Oslo, Oslo, N-0315, Norway*
[9]*Department of Electronic and Electrical Engineering University of Bath BA2 7AY, Bath, United Kingdom*
E-mail: zucca@astron.nl, rsharma@iitk.ac.in, div@ncra.tifr.res.in, div.oberoi@gmail.com, Eduard.Kontar@glasgow.ac.uk, john.morgan@csiro.au, peter.gallagher@dias.ie, sven.wedemeyer@astro.uio.no, b.forte@bath.ac.uk

The Solar, Heliospheric and Ionospheric (SHI) Physics Science Working Group of the Square Kilometre Array Observatory (SKAO) addresses the full chain of plasma processes linking the solar corona to the terrestrial environment. This overview chapter synthesises 16 topical contributions to *Advancing Astrophysics with the SKA – II*, spanning the quiet and active solar atmosphere, eruptive phenomena, heliospheric turbulence and solar-wind diagnostics, ionospheric science, stellar–solar connections, and the observational frameworks required to deliver these science goals. The primary focus is on the capabilities of Array Assembly 4 (AA4), the design baseline for both SKA1-Low (50–350 MHz) and SKA1-Mid (0.35–15.4 GHz), which together provide continuous spectral coverage, sub-arcsecond angular resolution, full-Stokes polarimetry, and sensitivity gains of an order of magnitude over existing facilities. From resolving fine-scale coronal heating events to mapping coronal mass ejection magnetic fields and characterising multi-scale heliospheric turbulence, SKAO will deliver transformative advances in solar and space-weather science. We frame these contributions as a single end-to-end Sun-to-Earth system. We identify cross-cutting themes and gaps not fully addressed by individual chapters and outline the staged roadmap from early operations through to the full AA4 capability.

1 Introduction and Scope

The Sun is the most powerful particle accelerator, the brightest radio source, and the dominant driver of space weather in our local cosmic environment. Understanding the physical processes that heat the million-degree corona, accelerate particles to relativistic energies, launch coronal mass ejections (CMEs), and shape the heliospheric plasma all the way to Earth's ionosphere remains among the central challenges in astrophysics. Radio observations occupy a privileged position in this endeavour: the emission mechanisms—thermal bremsstrahlung, gyroresonance and gyrosynchrotron radiation, and coherent plasma emission—provide diagnostics of coronal magnetic fields, electron energy distributions, and plasma turbulence that are inaccessible at other wavelengths.

The SKAO will deliver a step change in radio observing capability for SHI science. SKA1-Low, with 512 stations of 256 log-periodic dipole antennas spanning baselines up to ~65 km, covers 50–350 MHz and probes the corona and inner heliosphere from roughly 1.1 to >3 $R_\odot$. SKA1-Mid, comprising 197 dishes (133 SKA dishes plus 64 MeerKAT dishes) with baselines exceeding 150 km, covers 0.35–15.4 GHz in four receiver bands (Bands 1, 2, 5a, 5b), accessing the upper chromosphere, transition region, and low corona with sub-arcsecond resolution. Together, the two instruments provide continuous frequency coverage from 50 MHz to 15.4 GHz with full-Stokes spectropolarimetric imaging at cadences from milliseconds to hours.

This volume presents the science case against the design baseline Array Assembly 4 (AA4), with supplementary discussion of earlier array assemblies (AA*, AA2) and future enhancements. AA4 delivers the full collecting area, the densest instantaneous *uv*-coverage, and the design sensitivity—$A_{\rm eff}/T_{\rm sys} \sim 1000\,{\rm m^2\,K^{-1}}$ for SKA1-Low at 110 MHz and ~$1600\,{\rm m^2\,K^{-1}}$ for SKA1-Mid at 1.4 GHz—that underpin the science goals described in the following chapters.

The SHI contribution to *Advancing Astrophysics with the SKA – II* comprises 16 topical chapters that may be grouped as follows: the solar atmosphere, from the quiet corona through eruptive events (Mondal et al., 2026; Dey et al., 2026; Kontar et al., 2026; Sharma et al., 2026; Nakariakov et al., 2026; Patra et al., 2026; Kumari et al., 2026; Cheung et al., 2026; Kansabanik et al., 2026); heliospheric turbulence, solar wind, and energetic-particle transport (Chrysaphi et al., 2026; Zhang et al., 2026; Morosan et al., 2026); the ionosphere and geospace environment (Datta et al., 2026; Morgan et al., 2026); stellar connections (Mohan et al., 2026); and the underpinning observational, calibration, and data-analysis framework (Oberoi et al., 2026). This overview chapter serves as the editorial thread that links these contributions, provides a concise synthesis, identifies relevant gaps, and contextualises the collective effort within broader trends in heliophysics.

These topics form a single end-to-end Sun-to-Earth system, in which energy and disturbances propagate from coronal energy release (Section 2), through the turbulent heliosphere (Section 3), to their terrestrial imprint in the ionosphere (Section 4); the scientific dependencies are summarised in Figure 2.

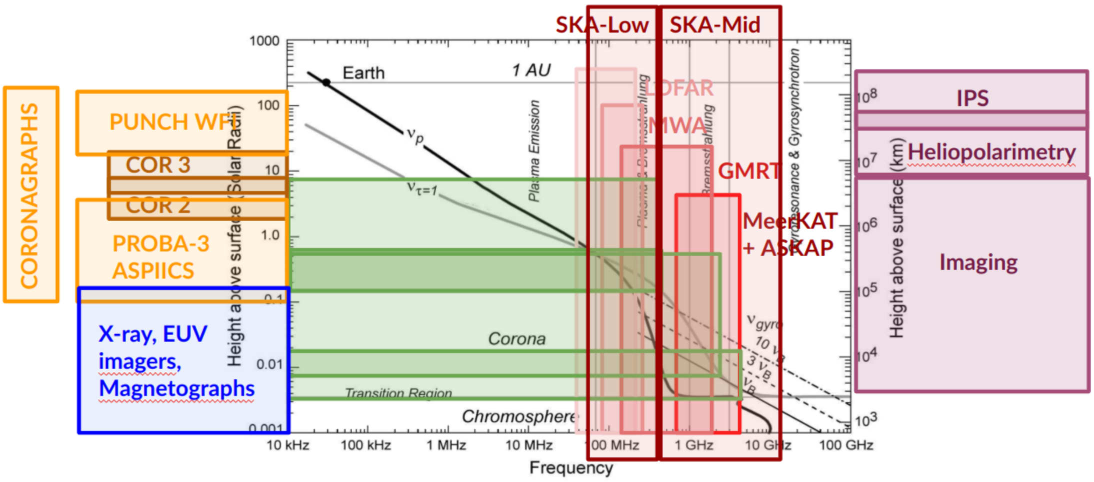

Figure 1: Frequency–height diagram for solar radio observations with SKA1-Low and SKA1-Mid. The shaded regions indicate the approximate coronal and heliospheric heights probed at each frequency via plasma emission (left axis), while the horizontal bars mark the receiver bands and the angular resolution achieved at AA4 baselines. Emission mechanisms transition from gyroresonance and bremsstrahlung at GHz frequencies to coherent plasma emission below ~300 MHz. Adapted from Gary & Hurford (2004).

2 Solar Atmosphere – From the Quiet Corona to Eruptive Events

2.1 Quiet Sun and Coronal Heating

One of the oldest unsolved problems in solar physics is the mechanism by which the corona is heated to temperatures exceeding 10^6 K. The nanoflare hypothesis, originally proposed by Parker (1988), posits that ubiquitous small-scale impulsive energy releases collectively supply the requisite energy budget. Recent observations with the Murchison Widefield Array (MWA) have provided the first radio evidence for pervasive weak, impulsive nonthermal emission from the quiet solar corona (Mondal et al., 2020; Sharma et al., 2022), consistent with this picture. Mondal et al. (2026) describe how SKAO's dramatic improvement in snapshot dynamic range (exceeding 10^5) and angular resolution at low frequencies will enable statistical studies of these faint transients across the full solar disk. By measuring the spectral and polarimetric properties of large populations of such events, SKAO will quantify their nonthermal energy content and directly test whether small-scale reconnection events can account for coronal heating. The order-of-magnitude sensitivity gain lowers the weak-event detection threshold by a comparable factor; given the steep event-energy power law, this yields population-scale samples that can measure the distribution slope—the decisive test of the nanoflare hypothesis.

2.2 Coronal Seeing and Sub-arcsecond Dynamics

Radio images of the Sun are broadened by scattering in the turbulent corona, an effect analogous to atmospheric seeing in optical astronomy. Dey et al. (2026) address this "coronal seeing" and its implications for high-resolution imaging with SKAO. Observations with LOFAR and the MWA have revealed that some sources—notably type-I noise-storm emission—are remarkably compact, with sizes as small as ~9 arcsec, far smaller than previously thought possible at metre wavelengths. Understanding the scattering kernel as a function of frequency, heliocentric distance, and heliographic position is essential for deconvolving intrinsic source structures from propagation-induced broadening. SKAO's long baselines and dense uv-coverage will simultaneously constrain scattering models and reveal fine structures in the corona that current instruments cannot resolve.

2.3 Solar Radio Burst Fine Structures

Solar radio bursts display a rich taxonomy of fine structures—narrowband spikes, stria bursts, zebra patterns, fibre bursts—that encode information about the microphysics of particle acceleration and the properties of the ambient plasma. Kontar et al. (2026) review the diagnostic potential of these features and the requirements for exploiting them with SKAO. Imaging spectroscopy with LOFAR has demonstrated that individual type-IIIb stria burst elements can be spatially and spectrally resolved (Kontar et al., 2017), but the limited uv-coverage restricts source characterisation. With SKA1-Low, the combination of sub-second time resolution, ~10 kHz spectral resolution, and imaging at arcminute to sub-arcminute scales will enable routine identification and physical modelling of fine structures across the full range of coherent emission processes.

2.4 Particle Acceleration in Solar Flares

Solar flares accelerate electrons and ions to high energies within seconds. The radio signatures of these nonthermal populations span the full SKAO frequency range: coherent plasma emission at low frequencies traces electron beams propagating through the corona, while incoherent gyrosynchrotron emission at GHz frequencies maps the energy distribution and pitch-angle anisotropy of trapped electrons in flaring loops. Sharma et al. (2026) demonstrate that SKA1-Mid Band 5 observations (4.6–15.4 GHz) will resolve the spatial structure of gyrosynchrotron sources in individual flaring loops with ~0.1 arcsec resolution, enabling spectral inversion to recover the magnetic field strength, nonthermal electron density, and energy spectral index as functions of position. When combined with SKA1-Low observations of the associated coherent emission and with hard X-ray data from missions such as Solar Orbiter STIX, SKAO will provide an end-to-end characterisation of the acceleration and transport of energetic electrons in flares.

2.5 Quasi-Periodic Pulsations

Quasi-periodic pulsations (QPPs) are a common feature of solar flare emission, observed across the electromagnetic spectrum from radio to gamma-rays. Their origin is debated: competing models invoke magnetohydrodynamic (MHD) oscillations of flaring structures, periodic or bursty reconnection, and nonlinear wave–particle interactions. Nakariakov et al. (2026) describe how SKAO will advance QPP research by observing simultaneously in both coherent and incoherent emission domains with continuous spectral coverage. The high time resolution ($\lesssim$50 ms) and sensitivity of SKAO will reveal QPP signatures in weak flares that are presently undetectable, while machine-learning methods applied to the high-cadence data streams will enable automated detection and classification of QPP events across the full activity cycle.

2.6 Coronal Magnetography

Direct measurement of the coronal magnetic field—the fundamental quantity governing coronal structure and dynamics—remains one of the principal observational challenges in solar physics. Radio observations offer two complementary pathways: gyroresonance emission, sensitive to the magnetic field strength in active-region loops at GHz frequencies, and circular polarisation of plasma emission at low frequencies, encoding the field in the emission and propagation regions. Patra et al. (2026) present the case for routine coronal magnetography using SKAO's spectropolarimetric capabilities. The exceptional polarisation purity of SKA1-Low and SKA1-Mid ($\lesssim$0.1% instrumental polarisation leakage after calibration) will enable Stokes-V measurements of thermal gyroresonance layers in active regions with SKA1-Mid and broadband circular-polarisation mapping of the quiet corona with SKA1-Low, together yielding magnetic-field maps from the low corona out to several solar radii. Resolving the SKA1-Mid gyroresonance layers recovers the coronal field to a few-percent precision, unlike optical/EUV magnetography, which extrapolates the photospheric field. At SKA1-Low frequencies the Stokes-V diagnostic is less direct, as it encodes both the emission and propagation regions; absolute field reconstruction there is model-dependent and requires propagation-aware forward modelling (Section 7).

2.7 Solar Radio Bursts: Metric to Kilometric

Type II, III, and IV radio bursts are the principal radio signatures of CMEs, flare-accelerated electron beams, and trapped energetic-particle populations, respectively. Their frequency drift rates, fine structures, and polarisation encode the kinematics and energetics of the driving phenomena as well as the density and magnetic-field profiles of the medium through which they propagate. Kumari et al. (2026) review SKAO's capability for comprehensive imaging spectroscopy of these bursts from metric to decametric wavelengths. SKA1-Low will image type II bursts driven by CME-associated shocks with sufficient angular resolution to locate the emission relative to the shock front, while type III burst imaging will trace electron-beam trajectories through the corona, constraining the three-dimensional magnetic topology.

2.8 Probing the Solar Corona with SKA-Mid

At GHz frequencies, the solar corona presents a wealth of fine-scale thermal and nonthermal structures—active-region loops, prominence–corona interfaces, microflare sites—that current instruments sample with limited spatial resolution and uv-coverage. Cheung et al. (2026) use forward-modelled MHD simulations to predict the radio appearance of the corona at SKA1-Mid frequencies and demonstrate that AA4 baselines will resolve structures at scales below 1 arcsec at 10 GHz. These capabilities are highly complementary to forthcoming EUV and optical facilities: the Multi-Slit Solar Explorer (MUSE; De Pontieu et al., 2022), the EUV High-Throughput Spectroscopic Telescope (EUVST), and the Daniel K. Inouye Solar Telescope (DKIST; Rimmele et al., 2020). Joint analysis of radio, EUV, and photospheric magnetogram data will enable self-consistent modelling of the thermal, nonthermal, and magnetic properties of the coronal plasma.

2.9 CME Magnetic Fields

The geoeffectiveness of a CME is determined largely by its internal magnetic-field configuration, a quantity that is extremely difficult to measure remotely. Kansabanik et al. (2026) describe two com-

Table 1: Comparison of imaging capabilities of selected solar instruments and radio facilities relevant to SHI science with SKAO. Values are representative; actual performance depends on observing mode, frequency, and target. Rows are grouped into dedicated solar facilities (which define the current operational baseline for solar radio imaging), general-purpose precursor/pathfinder arrays used for solar work, and SKAO (AA4). This grouping allows the reader to distinguish what is already routinely achievable at dedicated solar arrays from the capabilities SKAO uniquely adds.

Instrument	Waveband	Angular Res.	Cadence	Polarimetry
Optical/EUV solar context				
SDO/AIA	EUV (94–335 Å)	1.5″	12 s	No
SDO/HMI	6173 Å	1.0″	45 s	Full Stokes
DKIST/DL-NIRSP	500–1500 nm	0.1″	∼10 s	Full Stokes
Dedicated solar radio facilities (current operational baseline)				
EOVSA	1–18 GHz	∼3″	1 s	Dual circular
Nançay Radioheliograph	150–450 MHz	∼1–4′	0.1–1 s	Stokes I, V
MUSER	0.4–15 GHz	∼1.5–50″	∼25 ms	Dual circular
e-Callisto[c]	45–870 MHz	— (no imaging)	0.25 s	No
General-purpose precursor/pathfinder arrays				
MWA	80–300 MHz	∼2′	0.5 s	Full Stokes
LOFAR	10–240 MHz	∼3″[a]	0.01 s	Full Stokes
SKAO				
SKA1-Low(AA4)	**50–350 MHz**	**∼7″**	**≤0.05 s**	**Full Stokes**
SKA1-Mid (AA4)	**0.35–15.4 GHz**	**∼0.04″**[b]	**≤0.05 s**	**Full Stokes**

[a] International baselines; core-only resolution ∼2′.

[b] At 15 GHz with maximum AA4 baselines.

[c] Spectrometer network: high spectral/temporal coverage but non-imaging; listed for context.

plementary SKAO approaches. First, gyrosynchrotron emission from mildly relativistic electrons within the CME body provides a spectropolarimetric diagnostic of the magnetic-field strength and orientation out to $\sim 10\,R_\odot$ (Kansabanik et al., 2022). Second, Faraday rotation of linearly polarised background sources observed through the CME plasma constrains the line-of-sight magnetic field at larger heliocentric distances (Kooi et al., 2022). SKAO's wide field of view, large number of simultaneously observable polarised background sources, and spectropolarimetric sensitivity will transform CME magnetic-field measurement from isolated case studies into a systematic, operationally relevant capability. Because SKAO increases the number of polarised background sightlines per CME from one or a few to tens or hundreds, Faraday-rotation measurement becomes a tomographic reconstruction of the internal field—and hence the B_z governing geoeffectiveness—rather than a single detection.

Dedicated solar facilities already deliver either high angular resolution over a restricted band (EOVSA) or fast full-Sun spectral monitoring (Nançay, MUSER, e-Callisto), and thus define what is *already* achievable. SKAO is unique in combining all of these capabilities—sub-arcsecond-to-arcsecond imaging, continuous 50 MHz–15.4 GHz coverage, full-Stokes spectropolarimetry, and an order-of-magnitude sensitivity gain—simultaneously.

3 Heliosphere, Solar Wind, and Energetic Particles

Continuing the Sun-to-Earth chain, the eruptions, shocks, and beams of Section 2 now propagate through the turbulent heliosphere, which acts both as the next physical link and as a propagation filter on all radio waves crossing it.

3.1 Heliospheric Turbulence and Radio-Wave Propagation

The turbulent heliospheric plasma imprints observable signatures on radio waves propagating through it—angular broadening, intensity scintillation, temporal pulse broadening, and spectral modulation. These propagation effects are both a diagnostic of the turbulence itself and a source of distortion that must be understood to interpret solar radio observations correctly. Chrysaphi et al. (2026) present SKAO as a uniquely powerful probe of multi-scale heliospheric turbulence. The sensitivity gain over current instruments will allow the intrinsic properties of radio-burst sources to be cleanly separated from scattering-induced modifications for the first time, resolving long-standing discrepancies between observed and predicted source sizes. Simultaneously, the frequency dependence of the scattering signature will constrain the power spectrum and anisotropy of density fluctuations from spatial scales of tens of kilometres to solar radii, providing ground truth for heliospheric turbulence models.

3.2 Interplanetary Scintillation

Interplanetary scintillation (IPS)—the rapid intensity fluctuation of compact radio sources caused by the turbulent solar wind—has been used for decades to map the three-dimensional structure of the heliosphere. Morgan et al. (2026) discuss, among other topics, the potential for IPS studies with SKA1-Low and SKA1-Mid (the same contribution also treats the ionosphere, Section 4). The dramatically larger number of compact background sources detectable by SKAO ($>10^4$ within a few degrees of the Sun) will enable tomographic reconstruction of the solar-wind velocity, density, and turbulence with spatial resolution and cadence far exceeding current IPS arrays. CME-driven disturbances will be traceable through the inner heliosphere in near-real time, contributing directly to space-weather forecasting.

3.3 Angular Broadening and Radio Occultation

The angular broadening of compact radio sources observed at small elongation from the Sun is a powerful probe of coronal and heliospheric density turbulence. Zhang et al. (2026) demonstrate that the anisotropy of the angular broadening kernel encodes information about the magnetic-field topology: field-aligned density striations produce elongated scatter-broadened images whose orientation traces the projected field direction. Raja et al. (2026) complement this with a broader treatment of radio-wave propagation as a diagnostic of the coronal and solar-wind plasma, including group-delay and Doppler measurements from spacecraft-based and ground-based occultation experiments. SKAO will dramatically increase the density of background sources available for occultation and angular-broadening measurements, enabling continuous monitoring of coronal conditions across the solar cycle.

3.4 Solar Energetic Particles and Radio Associations

Solar energetic particle (SEP) events are a major space-weather hazard, yet the mechanisms by which particles are accelerated and released from the corona remain poorly understood. Morosan et al. (2026) address the intimate connection between SEP events and solar radio bursts: type III bursts mark electron-beam injection onto open field lines, type II bursts trace CME-driven shocks that accelerate particles, and the timing and spatial relationships between the two provide clues to the acceleration site and release conditions. SKAO's imaging capability will locate burst sources with arcsecond precision in the context of CME and shock structures observed by coronagraphs, while the spectral coverage will track emission from the low corona to the outer heliosphere. When combined with in-situ particle measurements from Solar Orbiter (Müller et al., 2020), Parker Solar Probe (Fox et al., 2016), and Aditya-L1, SKAO will close the gap between remote-sensing and in-situ observations of particle acceleration.

4 Ionosphere and Geospace Environment

The Sun-to-Earth chain closes at the ionosphere. Earth's ionosphere is both a science target and an instrumental challenge for low-frequency radio astronomy. Datta et al. (2026) show that radio interferometric arrays such as SKA1-Low measure total electron content (TEC) gradients with sensitivity exceeding that of Global Navigation Satellite System (GNSS) receivers by an order of magnitude, enabling characterisation of ionospheric structure on spatial scales from kilometres to hundreds of kilometres. The mid-latitude location of SKA1-Low in Western Australia (geomagnetic latitude $\sim -42°$) provides a complementary perspective to equatorial and high-latitude GNSS networks, and the continuous all-sky coverage during astronomical observations yields ionospheric data as a by-product.

Morgan et al. (2026) provide a comprehensive review of methods for observing and characterising the ionosphere with SKA1-Low, including direction-dependent calibration solutions that yield spatial maps of differential TEC, forward-modelling using physical ionospheric models, and the extraction of scintillation statistics. They emphasise the dual role of ionospheric science: as a research objective in its own right—studying travelling ionospheric disturbances, medium-scale structures, and the response to geomagnetic storms—and as a calibration requirement whose solution directly benefits all SHI (and indeed all low-frequency) science. Accurate ionospheric modelling will be critical during solar maximum, when ionospheric conditions at the SKA1-Low site may be significantly disturbed, and the Sun itself is the most scientifically productive target.

5 Stellar Connections and Broader Context

The Sun is the only star whose corona and activity cycle can be spatially resolved, but it is also just one exemplar of the diverse phenomena displayed by magnetically active cool stars. Mohan et al. (2026) explore the bridge between solar and stellar radio astrophysics, describing how SKAO will detect quiescent and flaring radio emission from M dwarfs and other active cool stars to distances of tens of parsecs. The direct SHI relevance is the Sun-as-a-star calibration: the spatially resolved solar measurements provide the ground truth needed to interpret disk-integrated stellar analogues of the same processes studied above. SKAO observations of the Sun as a spatially resolved "benchmark star" will calibrate the interpretation of unresolved stellar detections, while the stellar perspective will place solar activity in a broader evolutionary and environmental context. As broader context, the radio environment of a host star—driven by its magnetic activity, flaring rate, and wind properties—determines the space-weather conditions experienced by orbiting planets and may influence atmospheric retention and habitability.

6 Observational, Calibration, and Data-Analysis Frameworks

Realising the SHI science programme with SKAO demands an observational framework that is in many respects unique among SKA science cases. The Sun is an extremely bright, spatially extended, rapidly varying source that produces emission spanning many orders of magnitude in flux density. Oberoi et al. (2026) describe the state-of-the-art in solar radio observation, calibration, and imaging, drawing on the substantial body of experience accumulated with SKA precursors and pathfinders—principally the MWA and LOFAR, and more recently also MeerKAT. Key technical challenges include achieving snapshot dynamic range in excess of 10^5 against the bright solar disk, performing direction-dependent calibration in the presence of a dominant, time-variable extended source, and managing data rates that can exceed 10 TB hr^{-1} in spectropolarimetric imaging modes.

The chapter describes solutions that are being developed for AA4 operations: automated triggering of burst-mode observations using real-time observations, hierarchical data products that balance archival volume against scientific completeness, and integration with the SKAO Regional Centres (SRCs) for computationally intensive reprocessing. These frameworks are not SHI-specific in all respects; the calibration and imaging techniques for wide-field, high-dynamic-range, direction-dependent problems are broadly applicable across SKA science.

The standard SKAO/SRCNet model, oriented toward archival Observatory Data Products, provides the necessary calibration, imaging, and archival infrastructure but does not in its baseline form address solar-specific flux/polarisation calibration, high-cadence ($\lesssim$50 ms) burst imaging spectroscopy, or the near-real-time products required for space weather. A dedicated, low-latency SHI processing layer *upstream* of SRCNet is therefore likely needed; defining its interface is a pre-operations task (Section 7).

7 Cross-cutting Themes, Gaps, and the AA4 Outlook

Several themes recur across the individual chapters but are not fully addressed by any single contribution. We highlight these here both to acknowledge their importance and to motivate future work.

Real-time space-weather operations. Many of the science cases described above—CME magnetic-field measurement, type II burst tracking, IPS tomography—have direct relevance for operational space-weather forecasting. The transition from scientific analysis to real-time operational products requires dedicated pipelines with stringent latency constraints, robust automated quality control, and interfaces to existing space-weather services. While the potential is recognised in several chapters,

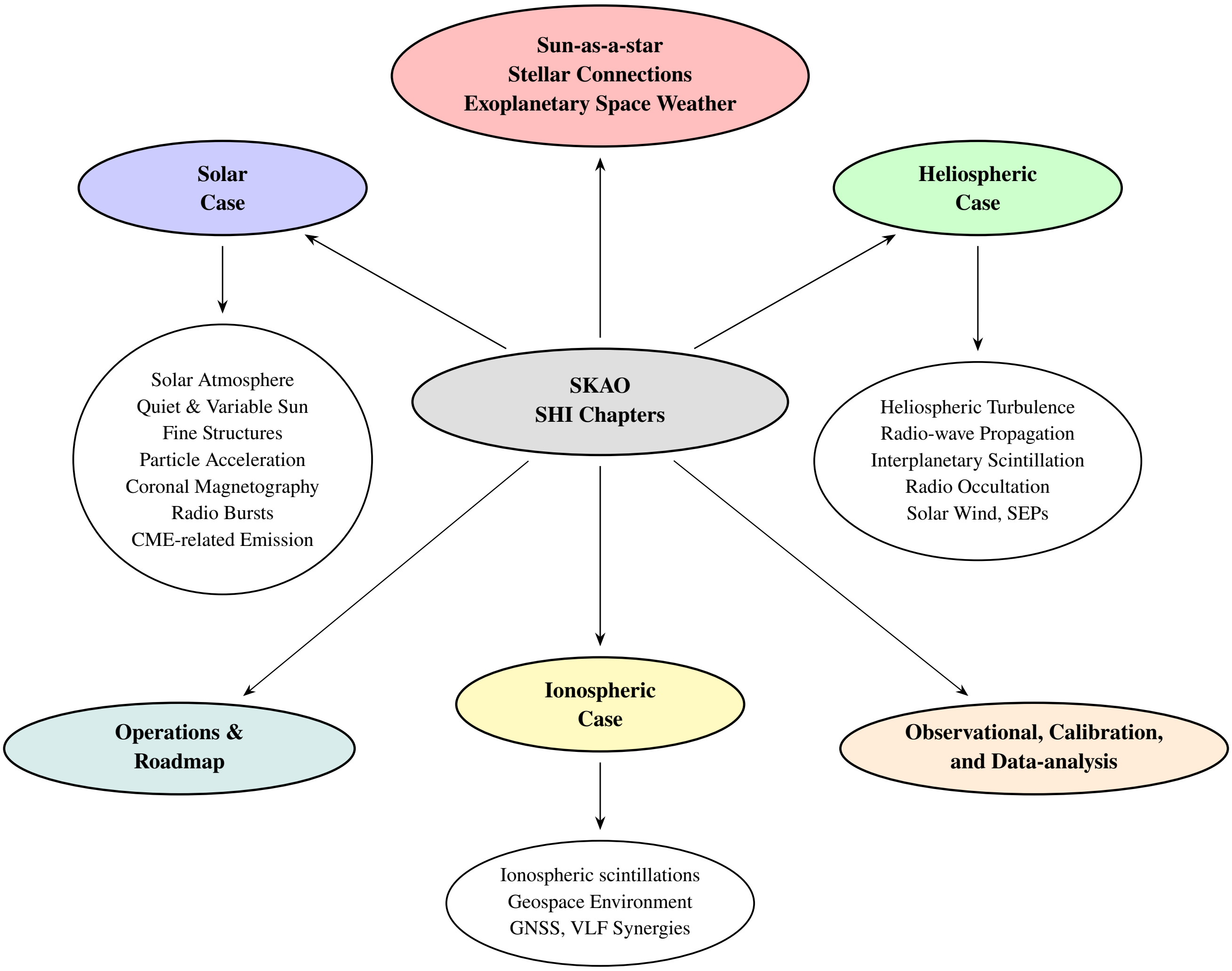

Figure 2: Overview of the 16 SHI topical chapters in *Advancing Astrophysics with the SKA – II* and their interconnections. Arrows indicate scientific dependencies (e.g., propagation effects discussed by Chrysaphi et al. 2026 affect the interpretation of solar burst observations in several other chapters). The observational framework chapter of Oberoi et al. (2026) underpins all SHI science.

the detailed architecture of a space-weather data stream from SKAO remains to be developed and would rely on the dedicated SHI processing layer of Section 6.

Multi-messenger and multi-mission coordination. SKAO will operate contemporaneously with an unprecedented fleet of heliophysics missions: Solar Orbiter, Parker Solar Probe, Aditya-L1 (Srivastava et al., 2021), PUNCH (Vourlidas et al., 2020), and PROBA-3, as well as ground-based facilities such as DKIST and the forthcoming MUSE and EUVST spectrographs. Coordinated observing campaigns that combine SKAO radio data with remote-sensing and in-situ measurements from these platforms will maximise the scientific return, but require planning frameworks, data-sharing protocols, and cross-calibration efforts that are still at an early stage.

Long-term synoptic monitoring. The solar cycle is a multi-decadal phenomenon, and many SHI science objectives—the statistical properties of coronal heating events, the evolution of the heliospheric turbulence spectrum, ionospheric climatology—benefit from continuous monitoring over a full activity cycle. Establishing a synoptic solar observing programme within the SKAO operational model, analogous to the routine monitoring performed by instruments such as SDO/AIA and GOES, will be important for long-term science return.

AA4 capabilities and the staged roadmap. The 16 chapters collectively demonstrate that the AA4 design baseline is sufficient to achieve transformative SHI science across the full range of topics considered here. The dense uv-coverage at AA4—512 stations for SKA1-Low and 197 dishes for SKA1-Mid—is critical for high-fidelity snapshot imaging of the extended, rapidly varying solar source. Full-Stokes imaging from 50 MHz to 15.4 GHz with millisecond time resolution and $\sim$10 kHz spectral resolution provides the spectropolarimetric parameter space needed for the diagnostic techniques described above. Early array assemblies (AA2, AA*) will already enable significant SHI science—particularly IPS, ionospheric studies, and observations of the brightest solar bursts—and will serve as essential pathfinding stages for commissioning solar observing modes and validating calibration strategies.

Community infrastructure. Delivering the SHI science programme at scale will require community-developed analysis pipelines, simulation tools for forward modelling of radio observables from MHD models, and integration with the SRC computing infrastructure. Investment in SHI-specific software tools—building on existing efforts for MWA and LOFAR solar data—and in training the next generation of solar radio astronomers are essential enabling activities.

Consistent forward modelling across SKA-Low and SKA-Mid. Forward modelling of radio observables is more developed for SKA1-Mid (Cheung et al., 2026) than for SKA1-Low, where scattering, angular broadening, and low-frequency magnetography rely on propagation effects not yet embedded in a common, polarisation-aware framework. Developing a SKA1-Low capability consistent with the SKA1-Mid one—and stating the associated assumptions and limitations—is a priority for the SHI programme.

8 Summary

The 16 topical chapters presented in this volume demonstrate that SKAO will be a transformative facility for solar, heliospheric, and ionospheric physics. From resolving the nonthermal signatures of nanoflare-scale coronal heating events (Mondal et al., 2026) to mapping the three-dimensional magnetic-field structure of CMEs (Kansabanik et al., 2026), from probing multi-scale heliospheric turbulence (Chrysaphi et al., 2026) to characterising ionospheric disturbances with unprecedented spatial resolution (Datta et al., 2026; Morgan et al., 2026), the science cases collectively define a programme of enormous breadth and depth tracing a single end-to-end Sun-to-Earth system.

The design baseline AA4 capabilities—sub-arcsecond resolution, full-Stokes spectropolarimetric imaging, sensitivity gains of an order of magnitude over existing facilities, and continuous spectral coverage from 50 MHz to 15.4 GHz—are well matched to the requirements articulated in each chapter. Cross-cutting challenges remain, notably in real-time space-weather data delivery, multi-mission coordination, long-term synoptic monitoring, and community software infrastructure; these represent important areas for further development as SKAO moves toward early science operations and the full realisation of AA4.

The SHI Science Working Group looks forward to a new era in solar and heliospheric radio physics with the SKAO, one that will deepen our understanding of fundamental plasma processes and strengthen our ability to predict and mitigate the space-weather hazards that increasingly affect our technological society.

References

M. C. Cheung et al. In *Advancing Astrophysics with the SKA – II (AASKAII)*. 2026. arXiv search: Report number AASKAII/Cheung01.

N. Chrysaphi et al. In *Advancing Astrophysics with the SKA – II (AASKAII)*. 2026. arXiv search: Report number AASKAII/Chrysaphi01.

A. Datta et al. In *Advancing Astrophysics with the SKA – II (AASKAII)*. 2026. arXiv search: Report number AASKAII/Datta01.

B. De Pontieu, P. Testa, J. Martínez-Sykora, et al. *The Astrophysical Journal*, 926:52, 2022. doi: 10.3847/1538-4357/ac4222.

S. Dey et al. In *Advancing Astrophysics with the SKA – II (AASKAII)*. 2026. arXiv search: Report number AASKAII/Dey01.

N. J. Fox et al. *Space Science Reviews*, 204:7–48, 2016. doi: 10.1007/s11214-015-0211-6.

D. Kansabanik, D. Oberoi, and S. Mondal. *The Astrophysical Journal*, 927:17, 2022. doi: 10.3847/1538-4357/ac4bba.

D. Kansabanik et al. In *Advancing Astrophysics with the SKA – II (AASKAII)*. 2026. arXiv search: Report number AASKAII/Kansabanik01.

E. Kontar et al. In *Advancing Astrophysics with the SKA – II (AASKAII)*. 2026. arXiv search: Report number AASKAII/Kontar01.

E. P. Kontar et al. *Nature Communications*, 8:1515, 2017. doi: 10.1038/s41467-017-01307-8.

J. E. Kooi et al. *Frontiers in Astronomy and Space Sciences*, 9:841866, 2022. doi: 10.3389/fspas.2022.841866.

A. Kumari et al. In *Advancing Astrophysics with the SKA – II (AASKAII)*. 2026. arXiv search: Report number AASKAII/Kumari01.

A. Mohan et al. In *Advancing Astrophysics with the SKA – II (AASKAII)*. 2026. arXiv search: Report number AASKAII/Mohan01.

S. Mondal, D. Oberoi, and A. Mohan. *The Astrophysical Journal*, 893:28, 2020. doi: 10.3847/1538-4357/ab7fab.

S. Mondal et al. In *Advancing Astrophysics with the SKA – II (AASKAII)*. 2026. arXiv search: Report number AASKAII/Mondal01.

J. Morgan et al. In *Advancing Astrophysics with the SKA – II (AASKAII)*. 2026. arXiv search: Report number AASKAII/Morgan01.

D. E. Morosan et al. In *Advancing Astrophysics with the SKA – II (AASKAII)*. 2026. arXiv search: Report number AASKAII/Morosan01.

D. Müller et al. *Astronomy & Astrophysics*, 642:A1, 2020. doi: 10.1051/0004-6361/202038467.

V. M. Nakariakov et al. In *Advancing Astrophysics with the SKA – II (AASKAII)*. 2026. arXiv search: Report number AASKAII/Nakariakov01.

D. Oberoi et al. In *Advancing Astrophysics with the SKA – II (AASKAII)*. 2026. arXiv search: Report number AASKAII/Oberoi01.

E. N. Parker. *The Astrophysical Journal*, 330:474–479, 1988.

D. Patra et al. In *Advancing Astrophysics with the SKA – II (AASKAII)*. 2026. arXiv search: Report number AASKAII/Patra01.

D. K. S. Raja et al. In *Advancing Astrophysics with the SKA – II (AASKAII)*. 2026. arXiv search: Report number AASKAII/Raja01.

T. R. Rimmele, M. Warner, S. L. Keil, et al. *Solar Physics*, 295:172, 2020. doi: 10.1007/s11207-020-01736-7.

R. Sharma, D. Oberoi, M. Battaglia, and S. Krucker. ApJ, 937(2):99, Oct. 2022. doi: 10.3847/1538-4357/ac87fc.

R. Sharma et al. In *Advancing Astrophysics with the SKA – II (AASKAII)*. 2026. arXiv search: Report number AASKAII/Sharma01.

A. K. Srivastava, A. N. Raghav, Z. I. Shaikh, et al. *Frontiers in Astronomy and Space Sciences*, 8:164, 2021.

A. Vourlidas, S. E. Gibson, R. A. Howard, et al. *Bulletin of the American Astronomical Society*, 52:306, 2020.

P. Zhang et al. In *Advancing Astrophysics with the SKA – II (AASKAII)*. 2026. arXiv search: Report number AASKAII/PeijinZhang01.